Biomaterials 34 (2013) 2787–2795

Contents lists available at SciVerse ScienceDirect

Biomaterials

journal homepage: www.elsevier.com/locate/biomaterials

In vivo biodistribution and toxicology of functionalized nano-graphene oxide in mice after oral and intraperitoneal administration

Kai Yang [a], Hua Gong [a], Xiaoze Shi [a], Jianmei Wan [b], Youjiu Zhang [b], Zhuang Liu [a,*]

[a] Jiangsu Key Laboratory for Carbon-Based Functional Materials & Devices, Institute of Functional Nano & Soft Materials Laboratory (FUNSOM), Soochow University, Suzhou, Jiangsu 215123, China
[b] School of Radiation Medicine and Public Health, Soochow University, Suzhou, Jiangsu 215123, China

ARTICLE INFO

Article history:
Received 30 November 2012
Accepted 1 January 2013
Available online 20 January 2013

Keywords:
Graphene
Biodistribution
Toxicology
Oral feeding
Intraperitoneal administration

ABSTRACT

Graphene oxide (GO) and its functionalized derivatives have attracted great attention in biomedicine in recent years. A number of groups including ours have studied the in vivo behaviors of functionalized nano-graphene after intravenous injection or inhalation, and uncovered the surface coating & size dependent biodistribution and toxicology profiles for this type of nanomaterials. However, the fate of GO derivatives in animals after oral feeding and intraperitoneal (i.p.) injection, which are two other major drug administration routes, remain unclear. Therefore, in this work, we sought to systematically investigate in vivo biodistribution and potential toxicity of as-made GO and a number of polyethylene glycol (PEG) functionalized GO derivatives with different sizes and surface coatings, after oral and intraperitoneal administration at high doses. It is found that ^{125}I labeled PEGylated GO derivatives show no obvious tissue uptake via oral administration, indicating the rather limited intestinal adsorption of those nanomaterials. In contrast, high accumulation of PEGyalted GO derivatives, but not as-made GO, in the reticuloendothelial (RES) system including liver and spleen is observed after i.p. injection. Further investigations based on histological examination of organ slices and hematological analysis discover that although GO and PEGylated GO derivatives would retain in the mouse body over a long period of time after i.p. injection, their toxicity to the treated animals is insignificant. Our work is an important fundamental study that offers a deeper understanding of in vivo behaviors and toxicology of functionalized nano-graphene in animals, depending on their different administration routes.

1. Introduction

The past several years have witnessed the explosion of graphene research in a variety of different fields, owing to the fascinating physical and chemical properties of this class of two-dimensional (2D) nanomaterials [1–7]. Regarding the use of graphene in biomedicine, there have been numerous reports to develop graphene-based biosensors aiming at detecting biomolecules with high sensitivities [8–13]. Owing to their ultra-high specific surface area, graphene and graphene oxide (GO) with appropriate surface functionalization can be used for drug and gene delivery [14–22]. The interesting intrinsic physical properties such strong light absorption and fluorescence of functionalized GO and its nanocomposites have also been utilized for photothermal therapy of cancer and as contrast agent for in vitro and in vivo imaging [17,23–31]. Moreover, graphene-based materials have recently shown promise as tissue engineering scaffolds for controlled growth and differentiation of several important classes of cells [32–37]. The exploration of graphene and its related nanomaterials in various directions of biomedicine are blooming nowadays.

Owing to the extensive use of graphene-based materials in academic research as well as the growing interests of applying them in the industry with large scales, the potential toxicity of graphene in biological systems has become a great concern [38–44]. It has been reported in a number of previous studies that pristine graphene or as-made GO without further surface modification after inhalation would cause severe pulmonary inflammation [39]. As-made GO after intravenous (i.v.) injection into mice would also accumulate in the lung, resulting in pulmonary edema and granuloma formation [45,46]. On the other hand, surface functionalized graphene or GO with improved water dispersity and better stability in physiological environments appear to be much less toxic [38,47].

* Corresponding author.
E-mail address: zliu@suda.edu.cn (Z. Liu).

0142-9612/$ – see front matter © 2013 Elsevier Ltd. All rights reserved.
http://dx.doi.org/10.1016/j.biomaterials.2013.01.001

Multu and co-workers found that although as-made GO after being directly administrated into the lungs of mice could induce mitochondrial generation of reactive oxygen spices (ROS) and inflammatory, Pluronic dispersed nano-graphene did not induce obvious lung injury at the same dose [39]. Our studies also found that nano-GO after being functionalized with hydrophilic non-toxic polymers such as polyethylene glycol (PEG) or dextran rendered no appreciable toxicity to mice after i.v. injection within 3 months at our tested dose (20 mg/kg) [47,48]. It was further noticed that the blood circulation half-lives and biodistribution profiles of nano-GO were dependent on their surface coatings and sizes [25].

The pharmacokinetics and toxicology of a drug are closely associated with its administration routes. Although researchers have gained substantial understanding regarding the behaviors and biological effects of GO and functionalized GO after inhalation and intravenous injection into mice, up to now, the in vivo biodistribution and toxicity of GO derivatives in animals via other different administration routes such as oral feeding and intraperitoneal (i.p.) injection remain unclear. Therefore, in this work, we want to systematically study the in vivo biodistribution and long-term toxicity of as-made GO and polyethylene glycol (PEG) coated GO functionalized by different ways, after oral and i.p. administration into healthy mice. We believe that our study would remarkably improve our understanding regarding the behaviors of functionalized graphene materials in animals.

2. Experimental section

2.1. Synthesis and characterization of PEGylated GO and its derivatives

Various PEGylated GO derivatives were prepared according to our previously reported protocols [25]. In brief, GO was produced from graphite by a modified hummer's method [16,17]. 6-arm-PEG was covalent conjugated to GO to form nGO-PEG. Excess PEG was removed by centrifugation filtration through 100 kDa molecular weight cut-off (MWCO) filters (Millipore). To prepared RGO and ultra-small nRGO, GO and nGO-PEG were reduced by hydrazine hydrate at 100 °C for 24 h. A PEG-grafted poly (maleic anhydride-alt-1-octadecene) (C18PMH–PEG) was synthesized following our previously reported procedure [25,49] and used to non-covalently functionalize RGO and nRGO to form RGO-PEG and nRGO-PEG. Excess polymers were removed by vacuum filtration through 0.1 μm filter membranes (Millipore). GO and PEGylated GO solutions were deposited on small pieces of silicon wafers and characterized by AFM (Veeco). The thicknesses of GO sheets were determined by the AFM measured heights, while the sheet sizes (diameter) were calculated by (length × width)$^{1/2}$.

2.2. ^{125}I labeling

nGO-PEG, RGO-PEG and nRGO-PEG were labeled by ^{125}I using a standard chloramine T oxidation method according to our established protocol [25,47]. 150 μl of PEGylated GO (2 mg/ml) was reacted with ~200 μCi $Na^{125}I$ and 100 μl of 4 mg/ml chloramine-T (Sigma–Aldrich) in pH 7.5 phosphate buffer (0.05 M) for 30 min at room temperature. Excess ^{125}I was removed by centrifuge filtration through Amicon filters (MWCO = 100 kDa) and washed with water for 4 times. A radiolabeling yield of ~50% was achieved.

2.3. Biodistribution

Female healthy balb/c mice orally and i.p. injected with ^{125}I-nGO-PEG, ^{125}I-RGO-PEG and ^{125}I-nRGO-PEG (100 μl of 20 μCi per mouse, a dose of 4 mg/kg) were sacrificed at 1, 7 and 30 days post injection, with major organs collected for radioactivity measurement using a gamma counter (Science and Technology Institute of China in Jia Branch Innovation Co., Ltd.).

2.4. Blood analysis and histology measurement

15 Healthy female balb/c mice were oral injected with nGO-PEG (100 mg/kg per mouse) and sacrificed at 1, 7 and 30 days p.i. (5 mice per time point). 80 Balb/c mice were i.p. injected with GO, nGO-PEG, RGO-PEG and nRGO-PEG (50 mg/kg per mouse) and sacrificed at 1, 7, 30, and 90 days p.i. (5 mice per time point). Other 20 balb/c mice were used as control groups and sacrificed at 1, 7, 30 and 90 days p.i. (5 mice per time points). Blood was collected from the orbital of treated mice for serum biochemistry assay and complete blood panel analysis, which were conducted by Shanghai Research Center for Biomodel Organism. Major organs from the treated mice were collected for hematoxylin & eosin (H&E) staining by the standard protocol and examined by a digital microscope (Leica QWin).

3. Results and discussion

PEGylation is possibly the most widely adopted technique to improve the biocompatibility of nanomaterials used in biomedicine. Our previous study has demonstrated that the blood circulation, biodistribution, and tumor targeting ability of PEGylated GO and reduced GO (RGO) are closely related to their surface coatings and sizes [25]. We thus decided to test several different PEGylated GO materials with varied sizes and surface chemistry in this study. According to our previously established protocol [16,17], GO produced from graphite by a modified Hummer's method was covalently functionalized with amine terminated six-arm branched PEG (10 kDa) to afford PEGylated nano-GO (nGO-PEG) with ultra-small sizes. To prepare PEGylated RGO with different sizes, as-made GO and nGO-PEG were both reduced by hydrazine hydrate to obtain RGO and nRGO, which were then non-covalently functionalized by a PEG-grafted poly (maleic anhydride-alt-1-octadecene) (C18PMH–PEG) polymer, offering RGO-PEG and nRGO-PEG, respectively, with the same surface coating but different sheet sizes [25,49](Fig. 1a). Atomic force microscope (AFM) was employed to characterize as-made GO, nGO-PEG, RGO-PEG and nRGO-PEG (Fig. 1b). From the AFM images, the average sheet diameters (assuming their shape to be round) of GO, nGO-PEG, RGO-PEG and nRGO-PEG were estimated to be 450, 25, 50 and 27 nm, respectively (Fig. 1c). nGO-PEG and nRGO-PEG thus had similar ultra-small 2D sizes (Fig. 1c). On the other hand, RGO-PEG and nRGO-PEG with non-covalent PEG coatings exhibited increased sheet thicknesses compared to nGO-PEG with the covalent PEGylation, suggesting that the surface PEG coating could be denser for the former two [25]. The average thickness of GO, GO-PEG RGO-PEG and nRGO-PEG was measured to be 0.94, 1.22, 4.43 and 5.66 nm, respectively (Fig. 1d). Three PEGylated GO derivatives all showed excellent stability in water, saline and fetal bovine serum (FBS), in marked contrast to as-made GO which readily aggregated in the presence of salts (Supporting information Figure S1).

In our previous work, we used ^{125}I to label three different PEGylated GO derivatives and studied their blood circulation and biodistribution in mice after intravenous injection. In this work, the same labeling strategy was applied to label nGO-PEG, RGO-PEG and nRGO-PEG with ^{125}I. The radiolabeling stability of three PEGylated GO derivatives in mouse plasma at 3 °C showed that less than 20% of ^{125}I was detached from the labeled materials within one week (Supporting information Figure S2). The reasonably good radiolabeling stability allows us to use this method for in vivo tracking, at least in short-term. However, this radiolabeling method was not applicable for as-made GO, which quickly precipitated in the labeling buffer containing a certain level of ions.

We first measured the in vivo biodistribution of ^{125}I labeled nGO-PEG, RGO-PEG and nRGO-PEG after oral feeding. Female balb/c mice were intragastrically injected with ^{125}I labeled nGO-PEG, RGO-PEG and nRGO-PEG (20 μCi/mouse), and sacrificed at 4 h and 1 day post injection (p.i.). The major organs were collected and measured by a gamma counter. At 4 h p.i., high levels of radioactivity were found in the stomach and intestine, but not in other major organs (Fig. 2). After 1 day, the ^{125}I levels became rather low in all the examined organs including stomach and intestine. Those data suggest that different types of PEGylated GO are not able to be adsorbed by the digestion system after oral feeding. The overall retained radioactivity levels in those mice were only 2~3% of the injected dose 1 day after administration, and became undetectable after one week, indicating the almost complete excretion of PEGylated GO after oral feeding.

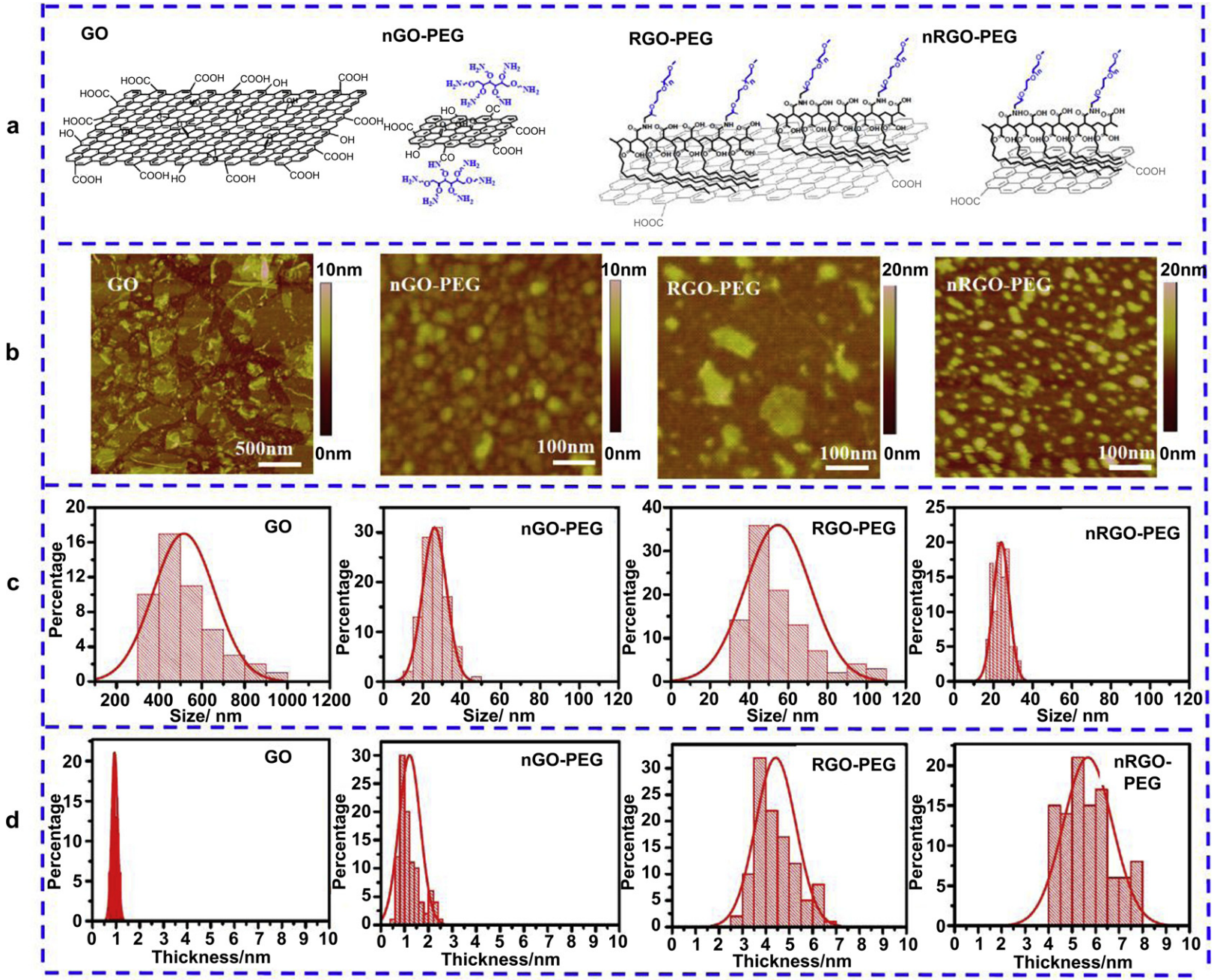

Fig. 1. Preparation and characterization of GO and PEGylated GO derivatives. (a) Schemes of GO, nGO-PEG, RGO-PEG and nRGO-PEG. (b) AFM images of GO, nGO-PEG, RGO-PEG and nRGO-PEG. (c&d) Statistics of sheet sizes (c) and thicknesses (d) of GO, nGO-PEG, RGO-PEG and nRGO-PEG samples based on AFM images.

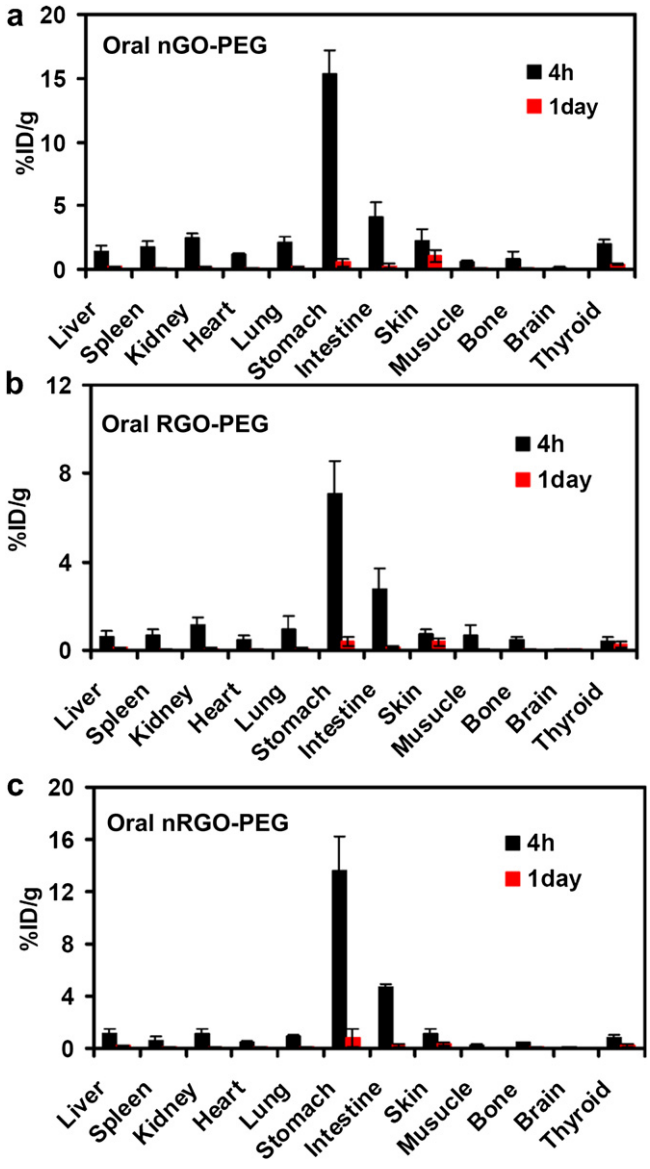

Fig. 2. The biodistribution of nGO-PEG (a), RGO-PEG (b), and nRGO-PEG (c) after oral administration. The results showed that ^{125}I labeled nGO-PEG, RGO-PEG, and nRGO-PEG could not be adsorbed by mouse organs and were rapidly excreted.

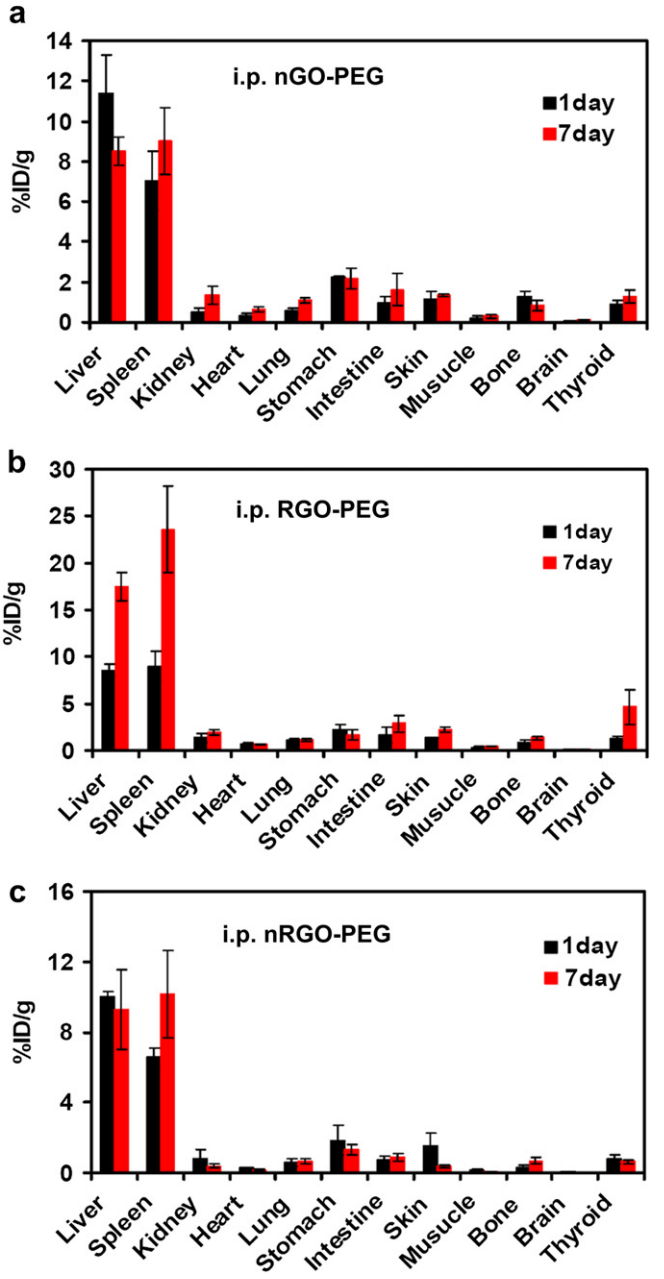

Fig. 3. The biodistribution of nGO-PEG (a), RGO-PEG (b), and nRGO-PEG (c) after i.p. administration. High RES uptake of PEGylated GO derivatives was noticed in the mouse liver and spleen following i.p. injection.

Meanwhile, we tested the in vivo biodistribution of ^{125}I labeled nGO-PEG, RGO-PEG and nRGO-PEG after i.p. administration. Female mice were i.p. injected with ^{125}I labeled PEGylated GO derivatives (20 μCi/mouse) and sacrificed after 1 and 7 days. Unlike those materials after oral feeding, all three types of PEGylated GO showed high accumulation in the mouse liver and spleen (Fig. 3), which are reticuloendothelial systems (RES) responsible for the clearance of foreign materials by macrophage uptake. Interestingly, RGO-PEG with larger sizes showed nearly 2-folds RES uptake compared to that of smaller nGO-PEG and nRGO-PEG at day 7, indicating that the size of nanomaterials could also be an important factor regulating the body adsorption of nanomaterials after i.p. injection.

We thus carefully studied the impacts of PEGylated GO derivatives to mice after i.p. injection. Mice i.p. injected with GO, nGO-PEG, RGO-PEG and nRGO-PEG at the dose of 50 mg/kg were scarified at 1, 7 and 30 days p.i. Consistent to the biodistribution results based on radioactivity measurement, we found that the color of liver and spleen in mice injected with nGO-PEG, RGO-PEG and nRGO-PEG changed from dark pink into black, directly evidencing the liver of uptake of PEGylated GO derivatives after i.p. injection (Fig. 4). Moreover, the color of liver and spleen kept black without any apparent change within 30 days, indicating the long retention time of nGO-PEG, RGO-PEG and nRGO-PEG in the mouse body after i.p. injection (Fig. 4). To our surprise, the color of liver and spleen in mice i.p. injected with as-made GO retained its dark pink color without a dramatic change compared to the untreated control (Fig. 4), suggesting that GO would be much less effectively adsorbed by the RES organs. This difference is likely owing to the poor physiological stability of as-made GO, which may aggregate instantly after i.p. injection to form large agglomerates that could not be adsorbed by the mouse organs. Black agglomerates were indeed found in the mouse abdominal cavity for animals injected

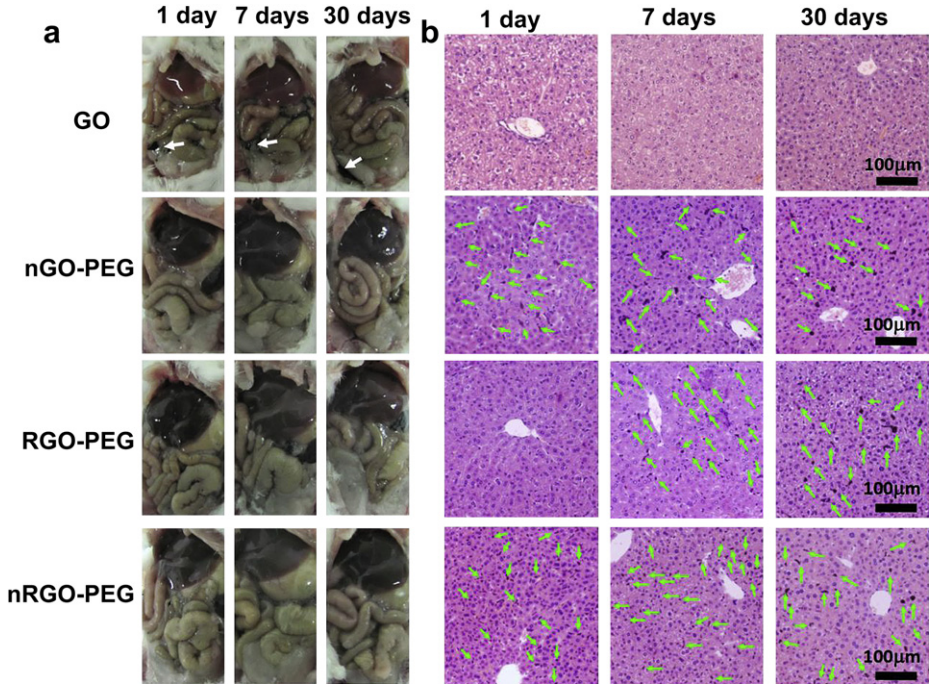

Fig. 4. The photos of dissected mice (a) and H&E stained liver slices (b) of mice i.p. injected with GO, nGO-PEG, RGO-PEG, and nRGO-PEG at the dose of 50 mg/kg. Mice were sacrificed at 1, 7 and 30 days p.i. While aggregated GO was found in the abdominal cavity (indicated by white arrows), the color of liver in mice treated with as-made GO did not show a significant change. No black dots were found in the liver slices of this group. In contrast, the color of liver turned into black in mice treated with nGO-PEG, RGO-PEG, and nRGO-PEG. Large numbers of black dots (highlighted by green arrows) were also noticed in their liver slices. (For interpretation of the references to color in this figure legend, the reader is referred to the web version of this article.)

with as-made GO over 30 days, but not for those injected with PEGylated GO derivatives at later time points (Fig. 4, highlighted by white arrows in the photo).

We then collected major organs of mice i.p. injected with GO and PEGylated GO derivatives at different time points for Hematoxylin and Eosin (H&E) staining and histological examination. For mice injected with nGO-PEG, large black brown dots ($\sim$10 μm in size), which were aggregated nanomaterials, were found in their liver slices as early as at day 1 after injection, and remained there even after 30 days. For mice injected with RGO-PEG and nRGO-PEG, the block dots were quite small at early time points (even not visible at day 1 for RGO-PEG injected mice), but grew larger later after 30 days. Those micrographs further confirm the RES uptake of PEGylated GO derivatives after i.p. injection. Although their exact body adsorption mechanism still needs further investigation, it is likely that the macrophages in RES organs could gradually engulf i.p. injected PEGylated GO derivatives. Consistent with the observation on the liver color, no obvious black dots were found in the liver of mice injected with as-made GO (Fig. 4). In H&E stained spleen slices from mice injected with PEGylated GO (data not shown), we also noticed some brown-black pigments, which, however, were relatively difficult to be differentiated from the stained spleen cell nuclei. Nevertheless, it is clear that while unfunctionalized GO which aggregates in physiological environments could not be effective adsorbed by the mouse body after i.p. injection, PEGylated GO with excellent dispersity would show significant uptake by RES organs such as liver and spleen.

In our previous work, we observed large numbers of black brown dots in the mouse liver after i.v. injection of nGO-PEG, and found a remarkable decrease in the number of black dots in the liver over time. Very few black dots were noticed in the mouse liver 20 days after injection, suggesting the obvious excretion of nGO-PEG from the mouse body. However, in this study, large numbers of black dots were still observed in the liver of mice i.p. injected with nGO-PEG, RGO-PEG and nRGO-PEG, even at 1 month p.i., suggesting the long-term retention of PEGylated GO in the mouse body after i.p. injection. Different from i.v. injected nGO-PEG, whose majority could accumulate in the liver and spleen from the circulating blood within the first few hours after injection, PEGylated GO derivatives after i.p. injection would be gradually adsorbed by the mouse body and slowly get accumulated in the RES organs. There possibly could be a balance between the gradual adsorption of PEGylated GO from the abdominal cavity into the liver, and the excretion of nanomaterials from the liver by biliary excretion [50,51], thus keeping the nanomaterials uptake in these organs at quite high levels over a long period of time, especially when the injected dose is rather high as that in our study. Obviously, the in vivo behaviors of nanomaterials are largely related to their administration routes.

Next, we studied whether various GO derivatives after oral feeding or i.p. injection would result in any toxicity to the treated mice. Owing to the limited oral bioavailability of three types of PEGylated GO, we then only chose nGO-PEG for toxicity study. Serum biochemistry and complete blood panel data revealed no apparent abnormality for mice fed with 100 mg/kg of nGO-PEG over a course of 30 days (Supporting Information Figure S3). Therefore, we conclude that nGO-PEG after oral feeding could not be adsorbed by the body and thus would not induce significant toxicity to the treated animals.

Since GO and PEGylated GO could retain inside the mouse body after i.p. administration for a long period of time, regardless of their RES adsorption, we carried out a more systematic study to look for in vivo potential long-term toxicity of GO derivatives after i.p. injection. Healthy female balb/c mice were i.p. injected with GO, nGO-PEG, RGO-PEG and nRGO-PEG at the dose of 50 mg/kg, and kept closely monitored over 3 months. No spontaneous animal

death or obvious body weight loss was observed within 90 days (Supporting information Figure S4). We then collected the major organs from mice treated with and without GO derivatives for H&E staining at various time points p.i. Neither obvious organ damage nor noticeable sign of inflammation was observed except the black brown dots found in the liver slices from mice injected with three types of PEGylated GO (Supporting information Figure S5).

We then carried out the serum biochemistry and complete blood panel assay for mice i.p. injected with GO, nGO-PEG, RGO-PEG and nRGO-PEG at 1, 7, 30 and 90 days post injection (5 mice per group, dose = 50 mg/kg). Blood from age-matched control untreated mice was also collected (5 mice per group). The liver function parameters including alanine aminotransferase (ALT) (Fig. 5a), alkaline phosphatase (ALP) (Fig. 5b), aspartate aminotransferase (AST) (Fig. 5c), and the ratio of albumin and globulin (A/G) (Fig. 5d), together with the parameter of kidney function, the blood urea nitrogen levels (BUN) (Fig. 5e), were tested in the serum biochemistry assay. No obvious hepatic or kidney toxicity, which is usually associated with elevated ALT, ALP and AST levels, was induced by i.p. injected PEGylated GO derivatives within 90 days. For GO treated mice, the ALT level at day 1 and ALP level at day 90 dropped to be slightly lower than the normal reference range. However, these differences were not physiologically significant in comparison to the untreated controls.

In the hematology analysis, the following important parameters were tested: white blood cell (WBC), red blood cell (RBC), hemoglobin (HGB), mean corpuscular volume (MCV), mean corpuscular hemoglobin (MCH), mean corpuscular hemoglobin concentration (MCHC), platelet count (PLT) and hematocrit (HCT) (Fig. 6 a–h). It was found that all the parameters in the treated groups appeared to be normal compared with the control group, expect the counts of WBC at day 7. It is well known that the housing environment, food and water could affect the level of WBC in mice. Considering the fact that GO and PEGylated GO injected mice at day 7 showed

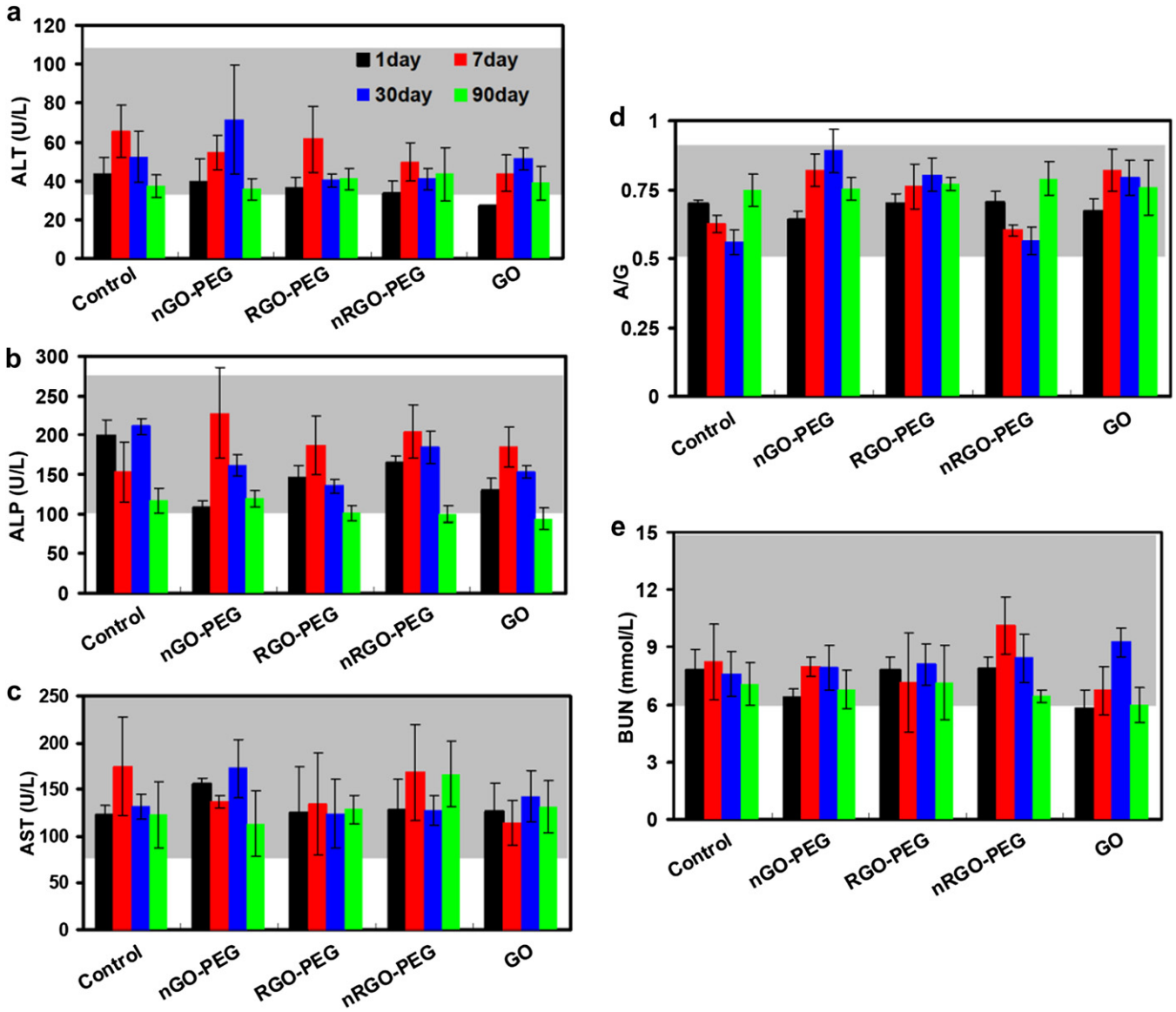

Fig. 5. The serum biochemistry analysis of female balb/c mice treated with GO, nGO-PEG, RGO-PEG, and nRGO-PEG at the dose of 50 mg/kg at 1, 7, 30 and 90 days p.i. Age-matched untreated mice were used as control groups. Alanine aminotransferase (ALT) (a), alkaline phosphatase (ALP) (b), aspartate aminotransferase (AST) (c), albumin/globin ratios (d) and blood urea nitrogen (BUN) (e) levels in the blood at various time points were tested. Serum biochemistry data did not uncover significant liver or kidney dysfunction induced by i.p. injected GO derivatives. Gray areas in the figures show the normal reference ranges of hematology data for healthy female balb/c mice [53].

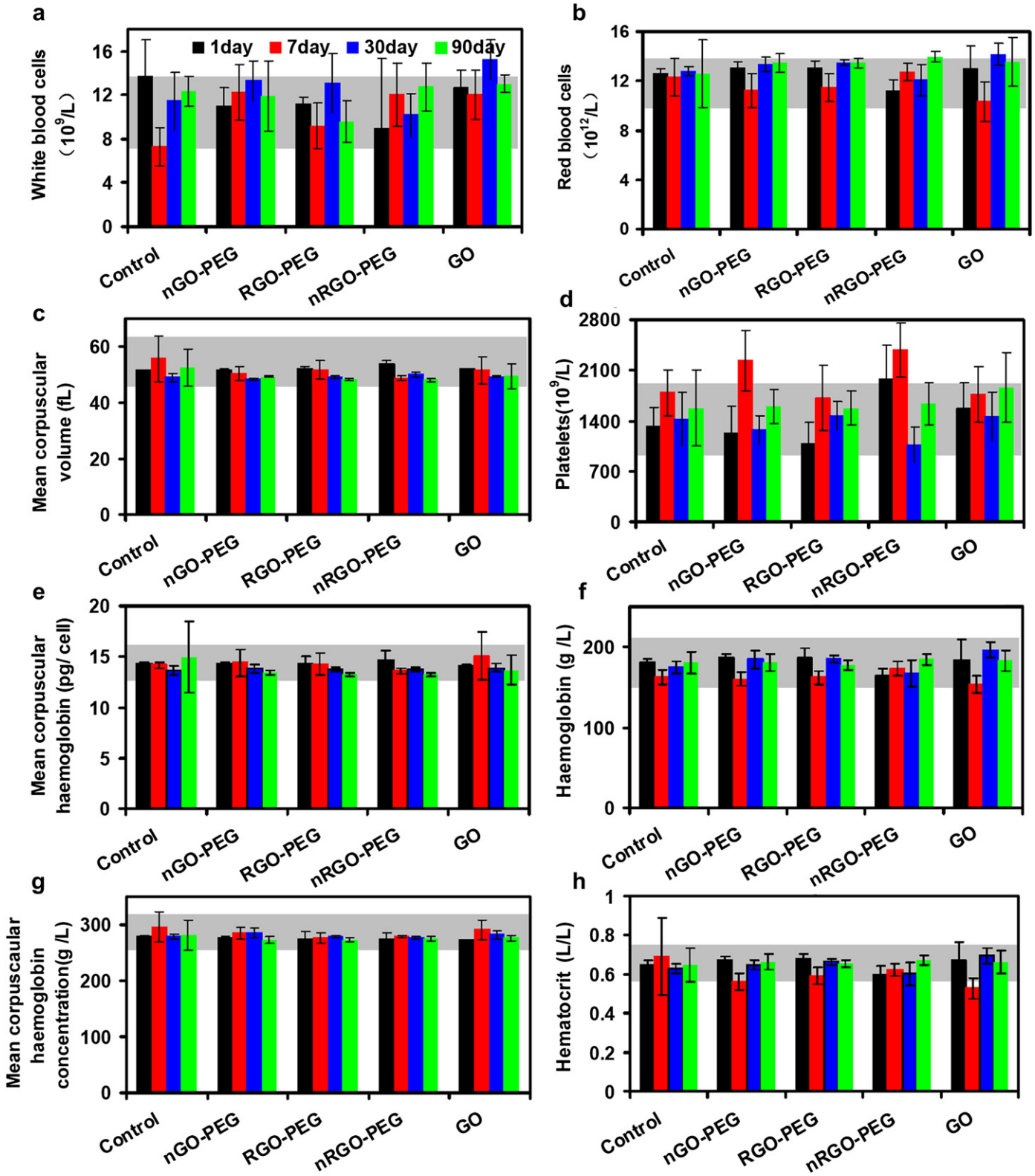

Fig. 6. The complete blood panel data from healthy control and treated mice. The following parameters were measured: white blood cells (a), red blood cells (b), mean corpuscular volume (c), platelets (d), mean corpuscular hemoglobin (e), hemoglobin (f), mean corpuscular hemoglobin concentration (g), and hematocrit (h). The majority of blood analysis data fell well within the normal ranges expect the WBC and PLT counts at a few time points for several treated groups, which, however, were not statistically significantly different in comparison to the respectively untreated control group. Error bars were based on five mice per group. Gray areas in the figures show the normal reference ranges of hematology data for healthy female balb/c mice [53].

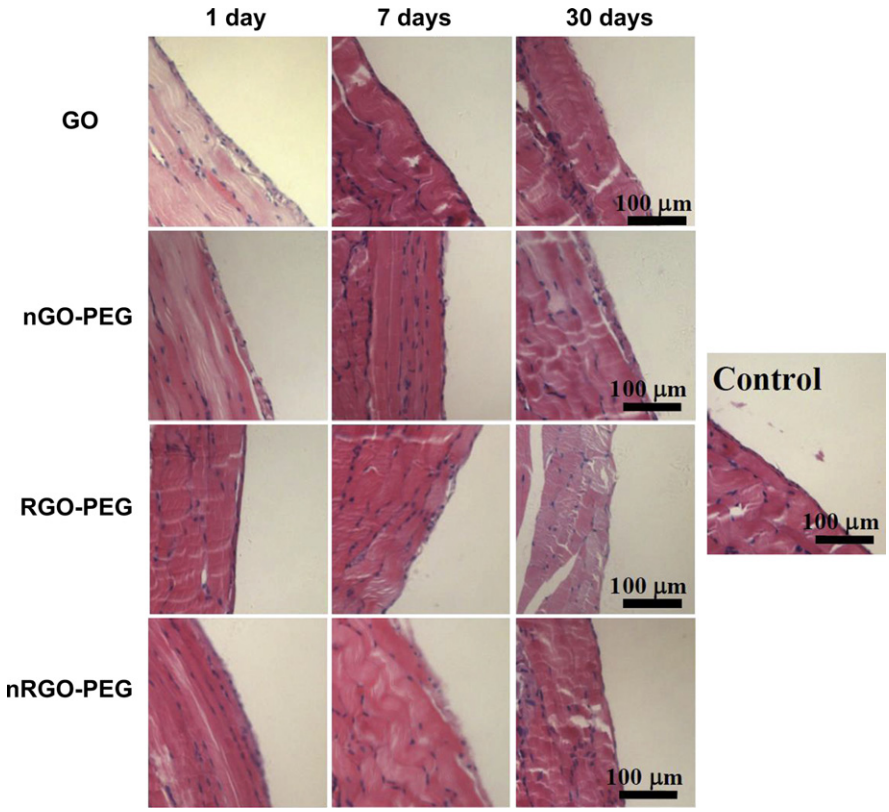

Fig. 7. The photos of H&E stained diaphragms slices from the mice treated with GO and PEGylated derivatives at 1, 7, 30 days p.i. No obvious granulamatous inflammation was observed in all treated groups.

similar WBC counts compared to control groups at day 1, 30, and 90, there might be some unusual housing condition for untreated control mice sacrificed at day 7. In addition, we also noted that the PLT counts in the blood of nGO-PEG and nRGO-PEG treated mice at day 7 were slightly out of the normal reference range. However, the differences between these groups versus the untreated control group at the same time point were not statistically significant (p value > 0.05).

In a previous work, Poland et al. have reported that long multiwalled carbon nanotubes (MWNTs) could induce granulomas formation in mice after i.p. injection within 7 days [52]. This observation has raised serious concerns on the possibility of carbon nanotubes to induce cancer. Therefore, in order to check whether GO derivatives would also induce granulomas formation, we collected the diaphragms from mice treated with GO, nGO-PEG RGO-PEG and nRGO-PEG at the high dose of 50 mg/kg, at 1, 7 and 30 days post i.p. injection for H&E staining. From the images of diaphragm slices, we did not observe any inflammation or granulomas formation in the diaphragms of treated mice within 30 days (Fig. 7). Thus, GO and PEGylated GO with much smaller sizes than MWNTs used in Poland's study were unlikely to induce granulomas formation in the abdominal cavity after i.p. injection.

4. Conclusions

In this work, we have systematically studied the in vivo behavior and long-term toxicity of GO and PEGylated GO derivatives after oral and i.p. injection. Our results showed that PEGylated GO derivatives after oral administration could not be adsorbed by organs and were rapidly excreted. In contrast, PEGylated GO derivatives, but not as-made GO, could be engulfed by phagocytes in the RES system after i.p. administration, by a size and surface coating related manner. Despite the long-term retention of i.p. injected GO and PEGylated GO in the mouse body, no significant toxicity was noticed in our systematic serum biochemistry, complete blood panel test, and histological analysis. The formation of granulomas, which could be induced by i.p. injected long MWNTs, was not observed in mice injected with high dose of GO or PEGylated GO. Our results suggest that the in vivo behaviors and toxicology of nanomaterials, including graphene, are closely associated with their surface coatings, size, and importantly, the administration routes.

Acknowledgments

This work was supported by the National Basic Research Program of China (973 Program, 2012CB932601 and 2011CB911002), National Natural Science Foundation of China (NSFC, 51222203, 51002100, 51132006), and a project funded by the Priority Academic Program Development of Jiangsu Higher Education Institutions (PAPD).

Appendix A. Supplementary data

Supplementary data related to this article can be found at http://dx.doi.org/10.1016/j.biomaterials.2013.01.001.

References

[1] Yang K, Feng L, Shi X, Liu Z. Nano-graphene in biomedicine: theranostic applications. Chem Soc Rev 2013;42:530–47.
[2] Loh KP, Bao Q, Ang PK, Yang J. The chemistry of graphene. J Mater Chem 2010;20:2277–89.
[3] Geim AK, Novoselov KS. The rise of graphene. Nat Mater 2007;6:183–91.
[4] Wang H, Robinson JT, Diankov G, Dai H. Nanocrystal growth on graphene with various degrees of oxidation. J Am Chem Soc 2010;132:3270–1.
[5] Dreyer DR, Park S, Bielawski CW, Ruoff RS. The chemistry of graphene oxide. Chem Soc Rev 2010;39:228–40.

[6] Huang X, Qi X, Boey F, Zhang H. Graphene-based composites. Chem Soc Rev 2011;41:666–86.
[7] Yan L, Zheng YB, Zhao F, Li S, Gao X, Xu B, et al. Chemistry and physics of a single atomic layer: strategies and challenges for functionalization of graphene and graphene-based materials. Chem Soc Rev 2012:97–114.
[8] Tang LA, Wang J, Loh KP. Graphene-based SELDI probe with ultrahigh extraction and sensitivity for DNA oligomer. J Am Chem Soc 2010;132:10976–7.
[9] He S, Song B, Li D, Zhu C, Qi W, Wen Y, et al. A graphene nanoprobe for rapid, sensitive, and multicolor fluorescent DNA analysis. Adv Funct Mater 2010;20:453–9.
[10] Akhavan O, Ghaderi E, Rahighi R. Toward single-DNA electrochemical biosensing by graphene nanowalls. ACS Nano 2012;6:2904–16.
[11] Jung JH, Cheon DS, Liu F, Lee KB, Seo TS. A graphene oxide based immunobiosensor for pathogen detection. Angew Chem Int Ed 2010;49:5708–11.
[12] Wen H, Dong C, Dong H, Shen A, Xia W, Cai X, et al. Engineered redox-responsive PEG detachment mechanism in PEGylated nano-graphene oxide for intracellular drug delivery. Small 2012;8:760–9.
[13] Huang P, Xu C, Lin J, Wang C, Wang X, Zhang C, et al. Folic acid-conjugated graphene oxide loaded with photosensitizers for targeting photodynamic therapy. Theranostics 2011;1:240–50.
[14] Feng L, Liu Z. Graphene in biomedicine: opportunities and challenges. Nanomedicine 2011;6:317–24.
[15] Feng L, Zhang S, Liu Z. Graphene based gene transfection. Nanoscale 2011;3:1252–7.
[16] Liu Z, Robinson JT, Sun XM, Dai HJ. PEGylated nanographene oxide for delivery of water-insoluble cancer drugs. J Am Chem Soc 2008;130:10876–7.
[17] Sun X, Liu Z, Welsher K, Robinson JT, Goodwin A, Zaric S, et al. Nano-graphene oxide for cellular imaging and drug delivery. Nano Res 2008;1:203–12.
[18] Zhang L, Xia J, Zhao Q, Liu L, Zhang Z. Functional graphene oxide as a nanocarrier for controlled loading and targeted delivery of mixed anticancer drugs. Small 2010;6:537–44.
[19] Tian B, Wang C, Zhang S, Feng L, Liu Z. Photothermally enhanced photodynamic therapy delivered by nano-graphene oxide. ACS Nano 2011;5:7000–9.
[20] Yang X, Zhang X, Ma Y, Huang Y, Wang Y, Chen Y. Superparamagnetic graphene oxide-Fe_3O_4 nanoparticles hybrid for controlled targeted drug carriers. J Mater Chem 2009;19:2710–4.
[21] Yang X, Zhang X, Liu Z, Ma Y, Huang Y, Chen Y. High-efficiency loading and controlled release of doxorubicin hydrochloride on graphene oxide. J Phys Chem C 2008;112:17554–8.
[22] Yang X, Wang Y, Huang X, Ma Y, Huang Y, Yang R, et al. Multi-functionalized graphene oxide based anticancer drug-carrier with dual-targeting function and pH-sensitivity. J Mater Chem 2011;21:3448–54.
[23] Robinson JT, Tabakman SM, Liang YY, Wang HL, Casalongue HS, Vinh D, et al. Ultrasmall reduced graphene oxide with high near-infrared absorbance for photothermal therapy. J Am Chem Soc 2011;133:6825–31.
[24] Yang K, Zhang S, Zhang G, Sun X, Lee ST, Liu Z. Graphene in mice: ultra-high in vivo tumor uptake and photothermal therapy. Nano Lett 2010;10:3318–23.
[25] Yang K, Wan J, Zhang S, Tian B, Zhang Y, Liu Z. The influence of surface chemistry and particle size of nanoscale graphene oxide on photothermal therapy of cancer using ultra-low laser power. Biomaterials 2012;33:2206–14.
[26] Narayanan TN, Gupta BK, Vithayathil SA, Aburto RR, Mani SA, Taha-Tijerina J, et al. Hybrid 2D nanomaterials as dual-mode contrast agents in cellular imaging. Adv Mater 2012;24:2992–8.
[27] Peng C, Hu W, Zhou Y, Fan C, Huang Q. Intracellular imaging with a graphene-based fluorescent probe. Small 2010;6:1686–92.
[28] Yang K, Hu L, Ma X, Ye S, Cheng L, Shi X, et al. Multimodal imaging guided photothermal therapy using functionalized graphene nanosheets anchored with magnetic nanoparticles. Adv Mater 2012;24:1868–72.
[29] Hu SH, Chen YW, Hung WT, Chen IW, Chen SY. Quantum-dot-tagged reduced graphene oxide nanocomposites for bright fluorescence bioimaging and photothermal therapy monitored in situ. Adv Mater 2012;24:1748–54.
[30] Hong H, Zhang Y, Engle JW, Nayak TR, Theuer CP, Nickles RJ, et al. In vivo targeting and positron emission tomography imaging of tumor vasculature with Ga-66-labeled nano-graphene. Biomaterials 2012;33:4147–56.
[31] Zhang Y, Nayak TR, Hong H, Cai W. Graphene: a versatile nanoplatform for biomedical applications. Nanoscale 2012;4:3833–42.
[32] Chen GY, Pang DWP, Hwang SM, Tuan HY, Hu YC. A graphene-based platform for induced pluripotent stem cells culture and differentiation. Biomaterials 2012;33:418–27.
[33] Nayak TR, Andersen H, Makam VS, Khaw C, Bae S, Xu X, et al. Graphene for controlled and accelerated osteogenic differentiation of human mesenchymal stem cells. ACS Nano 2011;5:4670–8.
[34] Kalbacova M, Broz A, Kong J, Kalbac M. Graphene substrates promote adherence of human osteoblasts and mesenchymal stromal cells. Carbon 2010;48:4323–9.
[35] Lee WC, Lim C, Shi H, Tang LAL, Wang Y, Lim CT, et al. Origin of enhanced stem cell growth and differentiation on graphene and graphene oxide. ACS Nano 2011;5:7334–41.
[36] Park SY, Park J, Sim SH, Sung MG, Kim KS, Hong BH, et al. Enhanced differentiation of human neural stem cells into neurons on graphene. Adv Mater 2011;23:263–7.
[37] Li N, Zhang X, Song Q, Su R, Zhang Q, Kong T, et al. The promotion of neurite sprouting and outgrowth of mouse hippocampal cells in culture by graphene substrates. Biomaterials 2011;32:9374–82.
[38] Singh SK, Singh MK, Kulkarni PP, Sonkar VK, Gracio JJA, Dash D. Amine-modified graphene thrombo-protective safer alternative to graphene oxide for biomedical applications. ACS Nano 2012;6:2731–40.
[39] Duch MC, Budinger GRS, Liang YT, Soberanes S, Urich D, Chiarella SE, et al. Minimizing oxidation and stable nanoscale dispersion improves the biocompatibility of graphene in the lung. Nano Lett 2011;11:5201–7.
[40] Yang K, Li Y, Tan X, Peng R, Liu Z. Behavior and toxicity of graphene and its functionalized derivatives in biological systems. Small 2013. http://dx.doi.org/10.1002/smll.201201417.
[41] Sanchez VC, Jachak A, Hurt RH, Kane AB. Biological interactions of graphene-family nanomaterials: an interdisciplinary review. Chem Res Toxicol 2012;25:15–34.
[42] Yan L, Wang Y, Xu X, Zeng C, Hou J, Lin M, et al. Can graphene oxide cause damage to eyesight? Chem Res Toxicol 2012;25:1265–70.
[43] Yan L, Zhao F, Li S, Hu Z, Zhao Y. Low-toxic and safe nanomaterials by surface-chemical design, carbon nanotubes, fullerenes, metallofullerenes, and graphenes. Nanoscale 2011;3:362–82.
[44] Li Y, Liu Y, Fu Y, Wei T, Le Guyader L, Gao G, et al. The triggering of apoptosis in macrophages by pristine graphene through the MAPK and TGF-beta signaling pathways. Biomaterials 2012;33:402–11.
[45] Wang K, Ruan J, Song H, Zhang J, Wo Y, Guo S, et al. Biocompatibility of graphene oxide. Nanoscale Res Lett 2011;6:8.
[46] Zhang X, Yin J, Peng C, Hu W, Zhu Z, Li W, et al. Distribution and biocompatibility studies of graphene oxide in mice after intravenous administration. Carbon 2011;49:986–95.
[47] Yang K, Wan JM, Zhang SA, Zhang YJ, Lee ST, Liu ZA. In vivo pharmacokinetics, long-term biodistribution, and toxicology of PEGylated graphene in mice. ACS Nano 2011;5:516–22.
[48] Zhang SA, Yang K, Feng LZ, Liu Z. In vitro and in vivo behaviors of dextran functionalized graphene. Carbon 2011;49:4040–9.
[49] Liu X, Tao H, Yang K, Zhang S, Lee ST, Liu Z. Optimization of surface chemistry on single-walled carbon nanotubes for in vivo photothermal ablation of tumors. Biomaterials 2011;32:144–51.
[50] Jani PU, Nomura T, Yamashita F, Takakura Y, Florence AT, Hashida M. Biliary excretion of polystyrene microspheres with covalently linked FITC fluorescence after oral and parenteral administration to male Wistar rats. J Drug Target 1996;4:87–93.
[51] Furumoto K, Ogawara K, Yoshida M, Takakura Y, Hashida M, Higaki K, et al. Biliary excretion of polystyrene microspheres depends on the type of receptor-mediated uptake in rat liver. Biochim Biophys Acta 2001;1526:221–6.
[52] Poland CA, Duffin R, Kinloch I, Maynard A, Wallace WAH, Seaton A, et al. Carbon nanotubes introduced into the abdominal cavity of mice show asbestos-like pathogenicity in a pilot study. Nat Nanotechnol 2008;3:423–8.
[53] Reference ranges of hematology data of healthy female Balb/c mice were obtained from Charles River Laboratories: http://www.criver.com/EN-US/PRODSERV/BYTYPE/RESMODOVER/RESMOD/Pages/BALBcMouse.aspx.